https://doi.org/10.1093/brain/awaf462 BRAIN 2026: 149; 668–679 | 668

BRAIN
ORIGINAL ARTICLE

Pioglitazone attenuates complement-mediated microglial synaptic engulfment in an Alzheimer's disease model

Juan Zu,[1,2,3,†] Cong Li,[3,4,†] Mochen Cui,[1,2,3,†] Xinwu Liu,[1,2] Zhouyang Pan,[1,2] Xiaohe Li,[1,2] Fang Zhang,[2] Johanna Gentz,[1] Gerda Mitteregger-Kretzschmar,[1] Jochen Herms[1,2,5,‡] and Yuan Shi[1,2,‡]

[†, ‡]These authors contributed equally to this work.

Synaptic loss is an early hallmark of Alzheimer's disease (AD), predominantly driven by aberrant microglial reactivity. Pioglitazone, a peroxisome proliferator-activated receptor gamma (PPAR-γ) agonist with anti-diabetic properties, has been shown to suppress microglial activity and improve cognitive performance in both AD models and clinical studies. However, whether its neuroprotective effects involve direct modulation of synaptic architecture remains unclear. Here, using longitudinal *in vivo* two-photon imaging, multi-channel immunohistochemistry, super-resolution confocal microscopy and three-dimensional reconstruction techniques in an AD mouse model, we analyse synaptic and microglial interactions.

We show that a 4-week pioglitazone treatment preserves dendritic spine density and enhances spine stability over time. Mechanistically, pioglitazone reduces synaptic C1q deposition, thereby limiting complement-mediated microglial synaptic engulfment and attenuating synapse loss.

These findings identify pioglitazone as a modulator of complement-dependent microglial synaptic pruning and support its therapeutic potential in preserving synaptic integrity during early AD pathogenesis.

1 Center for Neuropathology and Prion Research, Ludwig Maximilian University of Munich, Munich 81377, Germany
2 German Center for Neurodegenerative Diseases (DZNE), Munich 81377, Germany
3 Munich Medical Research School, Ludwig Maximilian University of Munich, Munich 80331, Germany
4 Department of Medicine IV, University Hospital, Ludwig Maximilian University of Munich, Munich 80331, Germany
5 Munich Cluster for Systems Neurology (SyNergy), Munich 81377, Germany

Correspondence to: Yuan Shi
Center for Neuropathology and Prion Research, Ludwig Maximilian University of Munich, Feodor-Lynen-Strasse 23, Munich 81377, Bavaria, Germany
E-mail: yuan.shi@med.lmu.de

Keywords: peroxisome proliferator-activated receptor-γ; pioglitazone; microglia; synaptic plasticity; Alzheimer's disease

Received August 28, 2025. Revised November 04, 2025. Accepted November 24, 2025. Advance access publication December 15, 2025
© The Author(s) 2025. Published by Oxford University Press on behalf of the Guarantors of Brain.
This is an Open Access article distributed under the terms of the Creative Commons Attribution License (https://creativecommons.org/licenses/by/4.0/), which permits unrestricted reuse, distribution, and reproduction in any medium, provided the original work is properly cited.

Downloaded from https://academic.oup.com/brain/article/149/2/668/8380271 by Deutsches Zentrum fur Neurodegenerative Erkrankungen DZNE user on 26 February 2026

Introduction

The cognitive decline in Alzheimer's disease (AD) is largely attributed to synaptic loss and dysfunction, which are closely linked to microglial function.[1-6] In recent years, a growing body of evidence has identified multiple mechanisms that contribute to microglia-mediated synaptic elimination, with the complement-dependent pathway being among the most thoroughly investigated. In both AD mouse models and human patients, the classical complement protein C1q has been observed as a key player in regulating synaptic loss.[3,7,8] As the initiating protein of the complement cascade within the innate immune system,[9] C1q preferentially tags and accumulates at vulnerable synapses within the diseased CNS.[3,7,8] This tagging leads to the deposition of the downstream complement protein C3, which subsequently activates C3 receptors on microglia.[8] The activation of these receptors triggers excessive microglial engulfment of synapses,[7,8] ultimately leading to neuronal loss.

Mitigating the abnormal microglial activation (a crucial component of neuroinflammation[10]) has long been a focus for AD treatment. Many anti-inflammatory drugs,[11] some not conventionally used for this condition, have been used in recent years as disease-modifying therapies for AD, including pioglitazone. Pioglitazone, an agonist for peroxisome proliferator-activated receptor gamma (PPAR-γ), is traditionally used for treating type 2 diabetes. In the CNS, pioglitazone has shown anti-inflammatory properties by promoting a shift in microglial activation towards a more neuroprotective phenotype.[12,13] In addition, earlier research suggested that pioglitazone promotes the performance of the AD mouse model in behavioural tasks related to learning and memory.[14,15] Despite the growing number of pioglitazone-related studies in AD therapy, most previous research has focused primarily on the ability of pioglitazone to suppress microglial pro-inflammatory properties. The specific mechanism by which pioglitazone affects synapses, in particular, whether and how pioglitazone modulates C1q-tagging at synapses, and its effects on subsequent synaptic loss, has not been clearly defined.

To address these questions, we used an AD mouse model, the *APPswe/PS1deltaE9* (*dE9*) strain,[16] and conducted both longitudinal *in vivo* two-photon imaging and super-resolution confocal imaging to monitor synaptic alterations in AD. Additionally, we used isolated synaptosomes and primary microglia, coupled with functional assays to decipher how pioglitazone influences these elements via C1q. Together, our findings revealed that pioglitazone significantly reduces C1q-tagging on synapses, dampens microglial phagocytic activity and stabilizes synaptic density during the early stages of AD pathology. These results provide new insights into the role of pioglitazone in synaptic regulation and highlight pioglitazone and the related PPAR-γ signalling pathway as potential therapeutic targets for mitigating complement-dependent microglial synaptic engulfment in AD.

Materials and methods

Animals

GFP-M transgenic mice (*Thy1-eGFP-M*), which express enhanced green fluorescent protein (eGFP) in sparse and random subsets of neurons within specific populations, were originally obtained from the Jackson Laboratory and maintained as heterozygotes. *APPswe/PS1deltaE9* (*dE9*) transgenic mice, which express human amyloid precursor protein (APP) harbouring the Swedish mutation (*K670N/M671L*) and a human presenilin-1 variant with a deletion of exon 9, resulting in accelerated amyloid-β (Aβ) deposition, were obtained from the Jackson Laboratory. To generate *APPswe/PS1deltaE9:Thy1-eGFP-M* mice, *APPswe/PS1deltaE9* mice were interbred with *Thy1-eGFP-M* (*GFP-M*) mice. All transgenic mice used in this study were bred on a C57BL/6J genetic background. The full official stock names of the mouse lines are listed in Supplementary Table 1. Both male and female transgenic mice, aged 4 months, were included in this study. The number of animals used in each experiment is specified in the corresponding figure legends. Mice were housed in the animal facility at the Center for Neuropathology, Ludwig Maximilian University of Munich, in specific pathogen-free conditions (21°C ± 1°C, 12 h light–12 h dark cycle) with *ad libitum* access to food and water. After surgery, each mouse was housed individually in a standard IVC Type II long cage. All animal procedures adhered to the regulations of the Ludwig Maximilian University of Munich and were approved by the Government of Upper Bavaria.

Drug administration

To evaluate the effects of pioglitazone on synaptic pathology *in vivo*, mice were randomly assigned to receive either a control diet or a treatment diet containing pioglitazone (350 ppm). Both diets were formulated and supplied by Ssniff Special Diets (Ssniff). Animals were allowed to feed *ad libitum* throughout the treatment period. Dietary intervention began at 4 months of age and continued for a total duration of 4 weeks, a time window corresponding to the early phase of amyloid-β plaque deposition and synaptic alterations in the *dE9* mouse model.

Cranial window implantation

The surgical procedure for cranial window implantation was performed as previously described.[17] In brief, mice underwent cranial window implantation under general anaesthesia [midazolam 5.0 mg/kg, fentanyl 0.05 mg/kg and medetomidine 0.5 mg/kg, intraperitoneally (i.p.)] and were placed in a stereotaxic frame. A 4 mm craniotomy was performed using a dental drill, followed by immediate placement of a 4 mm glass coverslip over the exposed cortex. The coverslip was sealed with dental acrylic, and a z-shaped headplate was affixed to the skull for subsequent imaging stabilization. After surgery, animals received carprofen (s.c.) and metamizole (i.g.), and were housed individually for 4 weeks prior to *in vivo* two-photon imaging.

Longitudinal *in vivo* two-photon imaging

Two-photon imaging was performed as previously described[17] on isoflurane-anaesthetized mice using a Zeiss LSM 7 MP microscope equipped with a 20× water-immersion objective. In brief, eGFP-expressing apical dendritic tufts from layer V pyramidal neurons were excited at 880 nm. Using ZEN software, *z*-stacks of 424 µm × 424 µm × 350 µm were collected at high resolution (0.83 µm in *xy*, 1 µm in *z*). Imaging sites were consistently relocated based on the distinct vasculature patterns. To label amyloid-β plaques *in vivo*, methoxy-X04 (1 mg/kg i.p.) was administered 24 h before imaging. Dendrites were aligned precisely to their original locations using baseline session data. Each imaging session lasted no more than 1 h.

Downloaded from https://academic.oup.com/brain/article/149/2/668/8380271 by Deutsches Zentrum fur Neurodegenerative Erkrankungen DZNE user on 26 February 2026

In vivo two-photon image processing and analysis of dendritic spines

To assess dendritic spine dynamics accurately, we restricted our analysis to spines that projected laterally and were clearly distinguishable within the imaging plane as previously described.[17] Manual classification was applied to each spine as either gained, lost or stable. Gained and lost spines were defined by their appearance or disappearance between two imaging sessions. Spines that maintained a consistent position (within 0.5 μm) across two or more sessions were deemed stable. Spine density was computed at each time point by dividing the number of spines by the dendritic segment length. For image processing, *z*-projections were generated from 3D stacks using Imaris (Andor Technology), which also allowed the removal of irrelevant neighbouring structures. The images were then deconvolved in AutoQuant X3 (Media Cybernetics), and contrast and brightness were manually adjusted.

Immunohistochemistry

Mice were deeply anaesthetized and transcardially perfused with cold phosphate buffered saline (PBS), followed by 4% formalin. Brains were post-fixed in 4% formalin for 24 h, then sectioned into 50-μm-thick slices for immunohistochemical analysis. Free-floating sections were permeabilized in 2% Triton X-100 overnight, then blocked for 4 h at room temperature in a solution containing 10% normal donkey serum, 2% bovine serum albumin or I-Block, and 0.3% Triton X-100 in PBS. Sections were incubated with primary antibodies (see Supplementary Table 1) at 4°C for 24 h, washed three times in PBS, and then incubated with secondary antibodies for 4 h at room temperature. Finally, sections were mounted with fluorescence medium (Dako, Germany). Images were captured using a Zeiss LSM 900 microscope equipped with Airyscan 2 (Zeiss) and a 63×/1.4 oil immersion objective.

Immunoblotting

Western blot analysis was performed to detect the expression levels of C1q (ThermoFisher Scientific), Proliferating Cell Nuclear Antigen (PCNA, Cell Signaling Technology), Stathmin (Cell Signaling Technology), Synaptophysin (Cell Signaling Technology) and Postsynaptic Density Protein 95 (PSD-95, Cell Signaling Technology) in mouse cortical tissue. Brain samples were stored at −80 °C until use. For protein extraction, tissues were homogenized in Triton X-100 lysis buffer (Alfa Aesar) supplemented with 1% phenylmethylsulfonyl fluoride and 2% phosphatase inhibitor cocktail and kept on ice throughout the procedure. The homogenates were centrifuged at 13 400*g* for 20 min at 4°C, and the resulting supernatants were collected for protein analysis. Protein concentrations were determined using a bicinchoninic acid assay kit and normalized to the same final concentration across all samples. Proteins were then separated by 10% SDS-PAGE (Bio-Rad) and transferred onto polyvinylidene fluoride membranes (Merck Millipore). Membranes were incubated overnight at 4°C with primary antibodies, followed by incubation with horseradish peroxidase-conjugated secondary antibodies for 2 h at room temperature. Protein bands were visualized by chemiluminescence, and signal intensities were quantified using Image Lab Software v.6.1 (Bio-Rad).

Super-resolution imaging and 3D analysis

Super-resolution confocal imaging was conducted using a Zeiss LSM 900 microscope equipped with Airyscan 2 and a Plan-Apochromat 63×/1.4 oil immersion objective. The super-resolution imaging parameters were optimized to achieve a lateral resolution of 0.035 μm per pixel and an axial resolution of 0.13 μm per pixel via the Airyscan 2 module. All obtained images were subjected to digital processing using the built-in 'Airyscan processing' algorithm. Processed images were then subjected to Imaris v.9.8.2 (Andor Technology) for 3D analysis. Microglia and lysosomes were reconstructed using the 3D Surface module, and PSD-95$^+$ puncta were visualized using the 3D Spot module. Quantification was performed by normalizing the number of lysosomal PSD-95$^+$ puncta to the total microglial volume, providing a precise measure of synaptic engulfment.

Primary microglia isolation and culture

Primary microglia were isolated using the Adult Brain Dissociation Kit (Miltenyi Biotec) following the manufacturer's instructions. Cortical tissues from adult wild-type (WT) mice were sectioned, enzymatically dissociated and processed via the gentleMACS Octo Dissociator (Miltenyi Biotec). The cells were then filtered, centrifuged and cleaned using debris and red blood cell removal solutions. The single-cell suspension was then incubated with CD11b MicroBeads and isolated using MACS LS columns on a QuadroMACS Separator (Miltenyi Biotec). The isolated microglia were then centrifuged and resuspended in a medium comprising DMEM/F12 (Gibco) with 10% fetal bovine serum (Gibco), 15 mM HEPES (ThermoFisher Scientific) and 1% penicillin–streptomycin (Gibco), supplemented with granulocyte-macrophage colony-stimulating factor (ThermoFisher Scientific) and glial cell derived neurotrophic factor (Sigma) at 10 ng/ml. Subsequently, microglia were plated on poly-D-lysine-coated glass coverslips in 24-well plates at a density of 1×10^5 cells per well.

Synaptosome purification and pHrodo conjugation

APPswePS1deltaE9 mice treated with either a pioglitazone or control diet were sacrificed, and cortical tissues were homogenized on ice in Syn-PER reagent (Thermo Fisher Scientific) supplemented with protease and phosphatase inhibitors. The homogenates were centrifuged at 1200*g* for 10 min, followed by 15 000*g* for 20 min to isolate synaptosomes. The synaptosomal pellets were then resuspended in fresh Syn-PER. For pHrodo labelling, synaptosomes were incubated with pHrodo Red (Thermo Fisher Scientific) in 0.1 M $NaHCO_3$ buffer (pH 8.5) at room temperature for 2 h. After labelling, the synaptosomes were washed and resuspended in PBS containing 5% dimethyl sulfoxide for subsequent experiments.

In vitro microglial engulfment assay

Primary microglia were cultured until day *in vitro* 5. For negative controls, cells were pretreated with 10 μM cytochalasin D for 1 h to inhibit phagocytosis. Subsequently, microglia were incubated with pHrodo-conjugated synaptosomes derived from either pioglitazone- or control-treated mice for 2 h at 37°C in 5% CO_2. After incubation, cells were sequentially washed, fixed, permeabilized, blocked and subjected to immunostaining before mounting. Imaging was performed using a Leica Stellaris 5 confocal microscope using a 63×/1.4 oil immersion objective, then deconvolved with the lightning module of LAS X software (Leica).

Downloaded from https://academic.oup.com/brain/article/149/2/668/8380271 by Deutsches Zentrum fur Neurodegenerative Erkrankungen DZNE user on 26 February 2026

Quantification of synaptosome engulfment was conducted using Imaris v.10.1.1 software (Andor Technology,). Internalized synaptosomes were identified as pHrodo$^+$ puncta within Iba1$^+$ microglia, and the data were normalized to the volume of Iba1-labelled microglial cytoplasm.

Statistics

All statistical analyses were performed using GraphPad Prism v.10 (GraphPad Software, USA). Repeated-measures two-way ANOVA with Bonferroni's multiple comparison test was applied to analyse time-series data from *in vivo* two-photon imaging. For normally distributed datasets, Student's two-tailed *t*-tests were used for two-group comparisons, and one-way ANOVA followed by Bonferroni correction was applied for analyses involving more than two groups. Statistical details of the ANOVA are provided in the figure legends, and *post hoc P*-values are reported in the corresponding graphs. All values are shown as the mean ± standard error of the mean, and a *P*-value of <0.05 was defined as statistically significant.

Results

Pioglitazone alleviates amyloid-associated synaptic pathology in an Alzheimer's disease mouse model

To model AD, we used the well-characterized *dE9* mouse strain. The model contains genes encoding both amyloid precursor protein (APP) with the Swedish mutation and presenilin 1 (PSEN1) with the deltaE9 mutation. This combination effectively recapitulates certain key aspects of amyloid pathology of AD.[18] In *dE9* mice, sparse amyloid-β plaques can be observed in cortical regions by 4–5 months of age, with synaptic decline emerging in the adjacent areas,[19] months before prominent neuronal death and extensive plaque accumulation.[18] Here, to investigate how pioglitazone might alleviate synaptic impairment, we used 5-month-old *dE9* mice, representing the early stage AD pathology in this model.

Initially, we assessed synaptic alterations caused by this AD pathology. To visualize synapses and trace their alterations longitudinally, we crossed *dE9* mice with *Thy1-eGFP-M* (*GFP-M*) transgenic mice, in which the green fluorescent protein (GFP) is expressed in a sparse subset of pyramidal neurons,[20] thereby enabling detailed morphological analysis of neuronal structures.

To explore how pioglitazone treatment might alter the structural plasticity of postsynaptic structures, i.e. dendritic spines, in ∼5-month-old *dE9:GFP-M* mice, we used *in vivo* two-photon microscopy. Through the pre-implanted cranial windows, we monitored changes in dendritic spines located in close proximity to amyloid-β plaques (<30 µm from plaques).

In vivo imaging of dendritic spines was performed both before and after a pioglitazone treatment period of 28 days (350 ppm in chew diet, *ad libitum*; Fig. 1A). As illustrated in Fig. 1B–E, in *dE9* mice, pioglitazone treatment significantly mitigated the decline in dendritic spines close to amyloid-β plaques. Specifically, treatment with pioglitazone led to a significant increase in the formation rate and a marked reduction in the elimination rate (Fig. 1F and G), thereby resulting in an overall elevation of spine density (Fig. 1E).

Furthermore, previous studies have shown that C1q tags and accumulates in vulnerable synapses, resulting in their phagocytosis by microglia.[8] To investigate the effect of pioglitazone on the vulnerability of dendritic spines in AD, we also traced the fate of individual dendritic spines across the 28 day period. Our findings demonstrated that stable spines, which were identified on Day 1 and still observable on Day 28, were elevated in *dE9* mice receiving pioglitazone treatment compared with those that did not receive the treatment (Fig. 1H and I).

In summary, our findings suggest that pioglitazone treatment can promote spine growth and enhance spine resistance to amyloid-β plaques. Jointly, these effects lead to an increased spine density and indicate better preservation of cognitive functions in the context of AD pathology.

Pioglitazone reduces microglial engulfment of synapses in Alzheimer's disease mice

Upon confirming the effects of pioglitazone on synapses, we explored further how pioglitazone affects the microglial engulfment of synapses, using both the ∼5-month-old *dE9* mice and age- and sex-matched WT mice.

To capture the synapses at a micrometre scale accurately, while preserving their spatial distribution within the microglia, we used multiplex immunostaining coupled with super-resolution microscopy and 3D reconstruction techniques.

As illustrated in Fig. 2A (middle and bottom), microglia accumulate around the amyloid-β plaques in the cortical regions of *dE9* mice. In comparison to the WT brains, microglia in *dE9* mice have a strongly elevated volume of CD68-labelled lysosomes (Fig. 2B), which notably contain higher levels of PSD-95-labelled postsynaptic puncta (Fig. 2C). This suggests an enhanced microglial engulfment of synaptic materials in the *dE9* mice.

Intriguingly, the 28 day pioglitazone treatment (350 ppm in chew diet, *ad libitum*) resulted in significant alterations in microglial behaviours. Specifically, while cycling around the amyloid-β plaque, microglia from pioglitazone-treated *dE9* mice exhibited reduced lysosome presence and fewer engulfed synaptic puncta (Fig. 2A–C). This leads to a promoted preservation of overall synaptic puncta in the *dE9* brain (Fig. 2D and E), suggesting an ameliorated AD pathology.

In addition, to assess the effects of pioglitazone on synaptic pruning in physiological conditions, we also examined microglial engulfment of synaptic materials in WT mice treated with either pioglitazone or vehicle. Our results revealed that microglia from pioglitazone-treated WT mice contained a comparable volume of CD68-labelled lysosomes to those from vehicle-treated WT mice. Although the levels of PSD-95$^+$ synaptic material were slightly elevated in pioglitazone-treated mice, this difference was not statistically significant (Supplementary Fig. 1). These findings suggest that pioglitazone treatment does not alter microglial phagocytosis of synaptic material in a normal CNS.

Collectively, these results suggest that pioglitazone treatment partly mitigates the abnormal microglial activity observed in *dE9* mice, particularly by reducing microglia-mediated synaptic loss.

Pioglitazone promotes synaptic preservation by reducing C1q-tagging

Upon confirming the effects of pioglitazone on both synapses and microglia, we proceeded to investigate whether and how pioglitazone regulates C1q. As previously noted, C1q plays a central role in AD-induced microglial engulfment of synapses.[8] Additionally, earlier research indicated that C1q promotes synaptic loss in a similar manner in inflammatory conditions. Given the anti-inflammatory properties of pioglitazone,[13] it is therefore plausible

Downloaded from https://academic.oup.com/brain/article/149/2/668/8380271 by Deutsches Zentrum fur Neurodegenerative Erkrankungen DZNE user on 26 February 2026

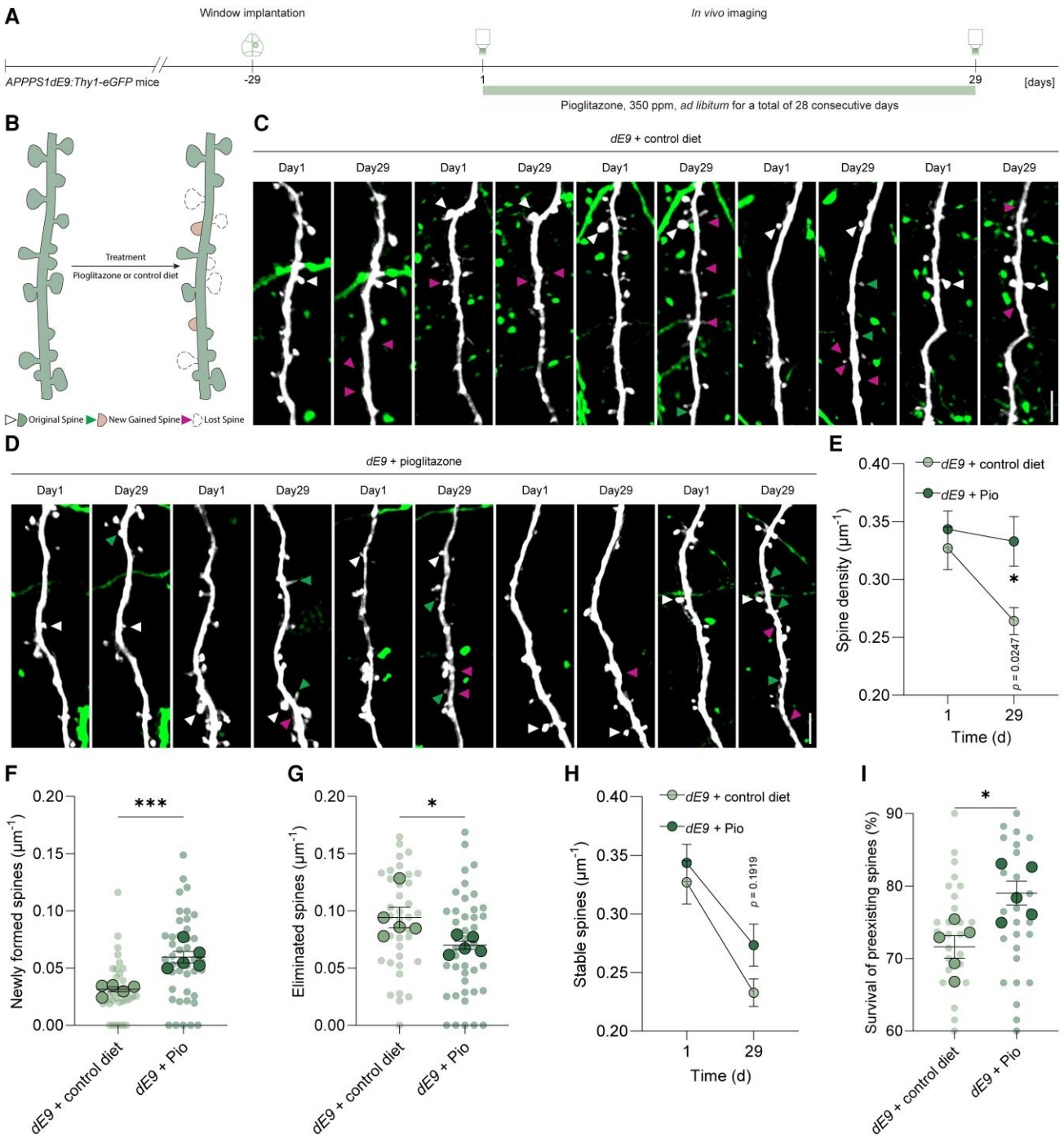

Figure 1 Pioglitazone alleviates amyloid-associated synaptic pathology in an Alzheimer's disease mouse model. (**A**) Experimental design schematic. (**B**) Illustration of dendritic spine structural plasticity. Arrowheads indicate stable (white), newly formed (green) or eliminated (magenta) spines. (**C** and **D**) Representative *in vivo* two-photon micrographs of apical dendritic tufts from *dE9* mice fed a control diet (**C**) or a pioglitazone-supplemented diet (**D**). (**E–G**) Quantification of dendritic spine density (**E**), spine formation (**F**) and elimination (**G**) following 28 days of pioglitazone or control diet treatment. (**H**) Density of stable spines after 28 days of treatment. (**I**) Survival rate of pre-existing spines over the 28 day period. $n = 5$ mice per group. Data are presented as the mean ± standard error of the mean. Two-way repeated-measures ANOVA followed by Bonferroni's multiple comparisons test [**E**: $F(1,8) = 26.02$, $P = 0.0009$; **H**: $F(1,8) = 6.341$, $P = 0.0359$]; two-sided unpaired Student's *t*-test [**F**: $t(8) = 5.227$, $P = 0.0008$; **G**: $t(8) = 2.518$, $P = 0.0359$; **I**: $t(8) = 3.260$, $P = 0.0115$]. $^{*}P < 0.05$, $^{***}P < 0.001$. Scale bars: 5 μm in **C** and **D**.

to hypothesize that the attenuation of this process might be attributed to alterations in C1q levels.

For this purpose, we assessed the C1q levels in the brains of *dE9* mice at ~5 months of age. As shown in Fig. 3A and B, the C1q levels in *dE9* brains are significantly higher than in WT brains. In line with our previous findings, 4 weeks of pioglitazone treatment (350 ppm in chew diet, *ad libitum*) drastically reduced the C1q density in *dE9* mice.

Given that the C1q-mediated synaptic loss is characterized by the formation of C1q deposition at the synapses[7,21] (i.e.

Downloaded from https://academic.oup.com/brain/article/149/2/668/8380271 by Deutsches Zentrum fur Neurodegenerative Erkrankungen DZNE user on 26 February 2026

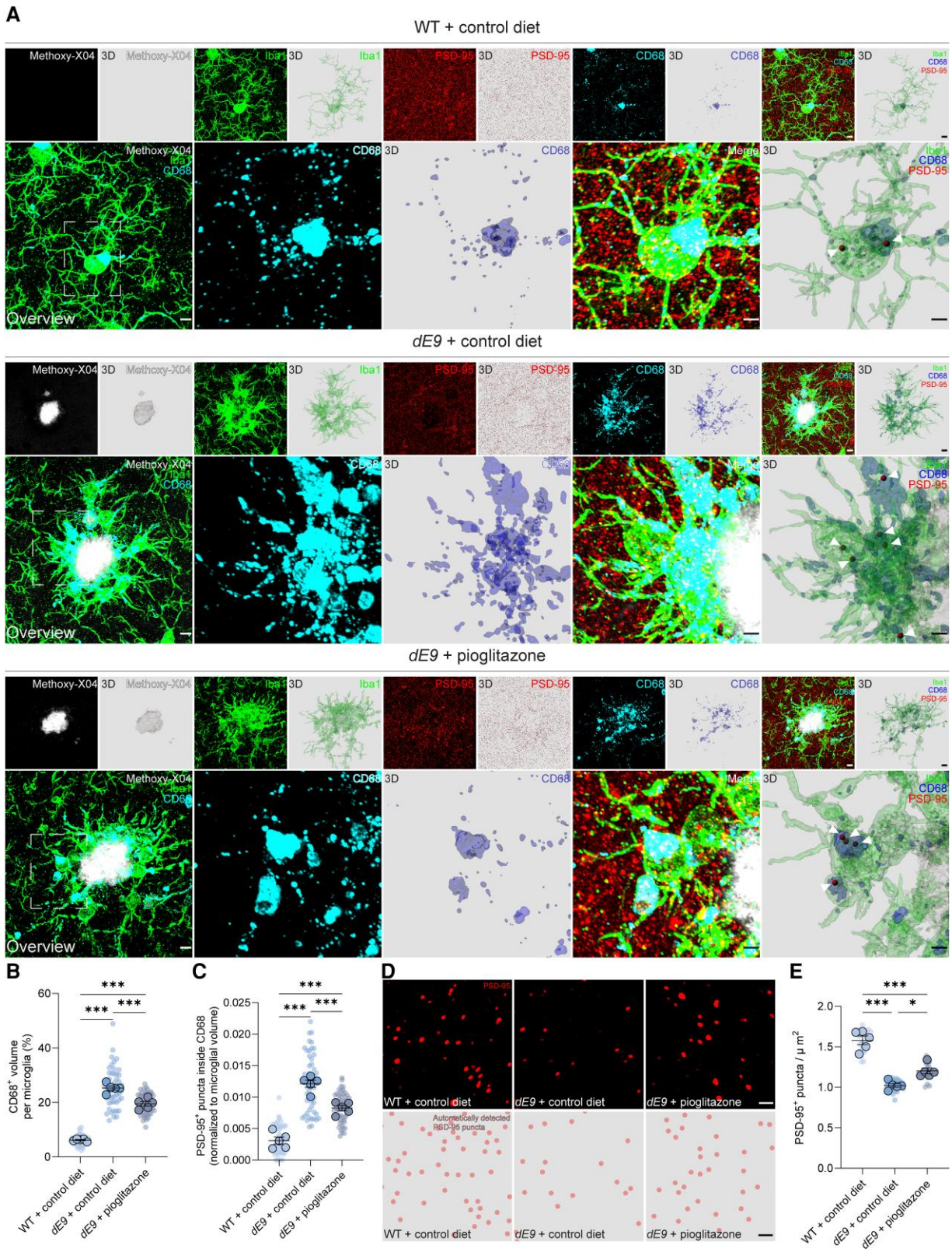

Figure 2 Pioglitazone reduces microglial engulfment of synapses in an Alzheimer's disease mouse model. (**A**) Representative super-resolution images and three-dimensional reconstructions of cortical microglia from ~5-month-old wild-type (WT), *dE9* and pioglitazone-treated *dE9* mice. In *dE9* mice, microglia cluster around amyloid-β plaques and display enlarged CD68$^+$ lysosomes that contain engulfed postsynaptic PSD-95$^+$ puncta . (**B** and **C**) Quantification of CD68$^+$ lysosomal volume (**B**) and the number of PSD-95$^+$ puncta engulfed by microglia (**C**) across groups (WT + control diet, *dE9* + control diet, and *dE9* + pioglitazone). (**D** and **E**) Representative confocal images and Imaris-based detection of PSD-95$^+$ postsynaptic puncta in the cortex (**D**) and corresponding quantification (**E**) in the same three groups. $n = 5$ mice per group. Data are presented as the mean ± standard error of the mean. One-way ANOVA followed by Bonferroni's multiple comparisons test [**B**: $F(2,12) = 220.5$, $P < 0.001$; **C**: $F(2,12) = 75.87$, $P < 0.001$; **E**: $F(2,12) = 51.21$, $P < 0.001$]. $^*P < 0.05$, $^{***}P < 0.001$. Scale bars: 5 µm in **A** (*full view*), 2 µm in **A** (*zoomed-in regions*) and 5 µm in **D**.

Downloaded from https://academic.oup.com/brain/article/149/2/668/8380271 by Deutsches Zentrum fur Neurodegenerative Erkrankungen DZNE user on 26 February 2026

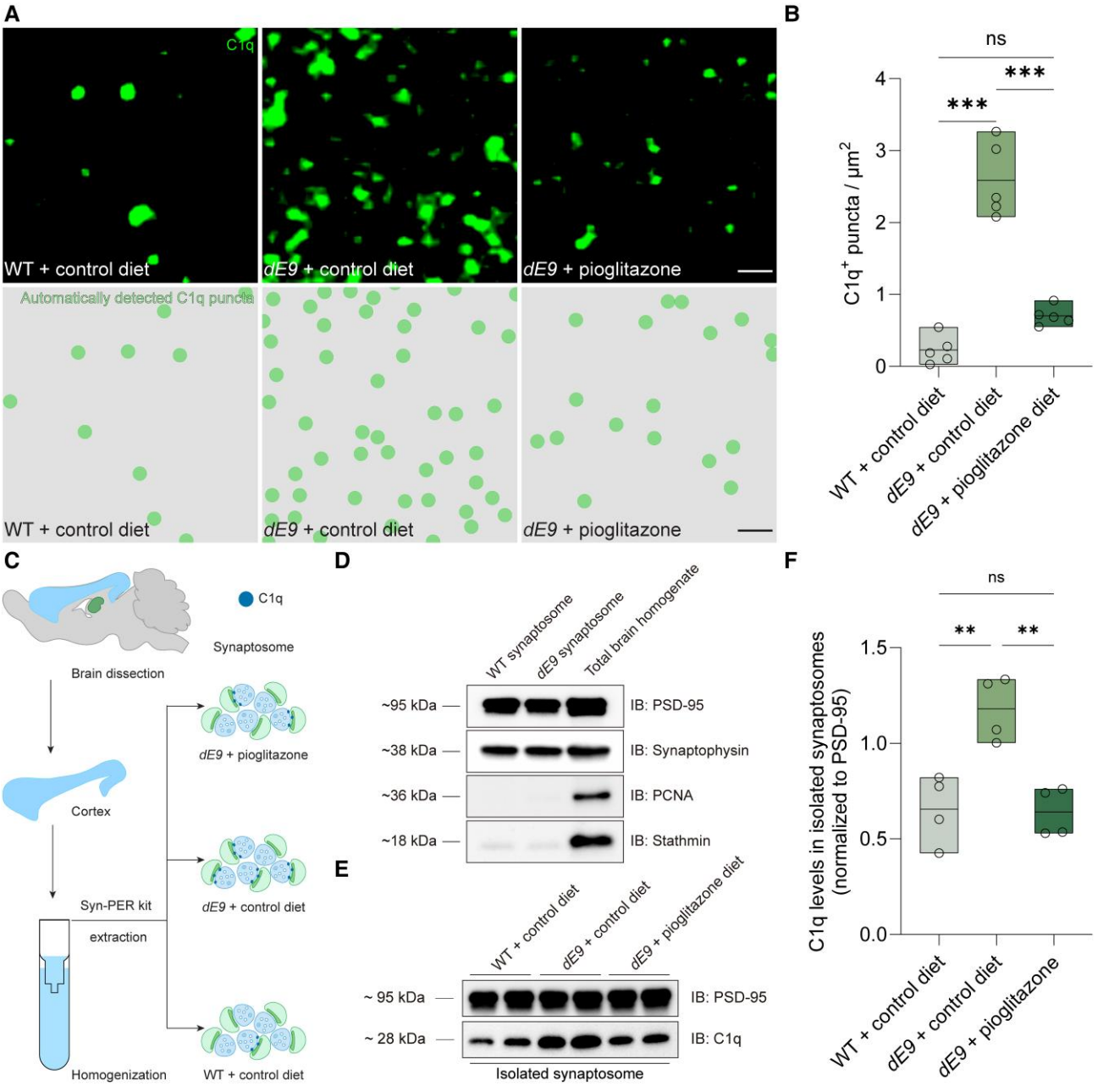

Figure 3 Pioglitazone reduces C1q accumulation and synaptic C1q-tagging in *dE9* mice. (**A** and **B**) Representative confocal images (**A**) and Imaris-based quantification (**B**) of C1q$^+$ puncta in the cortex of wild-type (WT) mice, *dE9* mice and pioglitazone-treated *dE9* mice. (**C**) Schematic overview of synaptosome isolation from mouse cortex. (**D**) Characterization of isolated synaptosomes used in microglial phagocytosis assay. Purity was validated by enrichment of pre- and postsynaptic proteins (synaptophysin and PSD-95), minimal presence of cytosolic protein (stathmin) and absence of nuclear protein (PCNA), compared with whole brain homogenate. (**E** and **F**) Representative immunoblot of C1q in cortical synaptosome fractions from WT, untreated *dE9* and pioglitazone-treated *dE9* mice, with PSD-95 used as a loading control (**E**) and corresponding quantification (**F**). $n = 5$ mice per group (**A** and **B**); $n = 4$ mice per group, with samples immunoblotted in triplicate (**E** and **F**). Data are presented as the mean ± standard error of the mean. One-way ANOVA followed by Bonferroni's multiple comparisons test [**B**: $F(2,12) = 70.66$, $P < 0.001$; **F**: $F(2,9) = 14.67$, $P = 0.0015$]. $^{**}P < 0.01$, $^{***}P < 0.001$. ns = no significant difference. Scale bars: 1 µm in **A**.

C1q-tagging), We subsequently evaluated the concentration of C1q within the synaptic materials, both with and without pioglitazone treatment.

We extracted synaptic terminals (synaptosomes) from the cortex of ~5-month-old WT mice and from both pioglitazone-treated and untreated *dE9* mice. To confirm the purity of the synaptosome preparations, we validated the absence of nuclear and cytoplasmic proteins, i.e. PCNA and stathmin, respectively (Fig. 3C and D). We then assessed the C1q content in these synaptosomes. As expected, compared with WT synaptosomes, synaptosomes isolated from pioglitazone-untreated *dE9* mice contain higher levels of C1q. Conversely, in *dE9* mice treated with pioglitazone, a significant reduction in synaptosomal C1q was observed (Fig. 3E and F).

In addition, to support our *ex vivo* findings described above, we performed functional assessments to determine how

Downloaded from https://academic.oup.com/brain/article/149/2/668/8380271 by Deutsches Zentrum fur Neurodegenerative Erkrankungen DZNE user on 26 February 2026

synaptosomes from different mice led to distinct microglial responses. To monitor the engulfment of synaptosomes, we conjugated them with pHrodo, a pH-sensitive dye that emits a fluorescent signal upon lysosomal engulfment (Fig. 4A). Furthermore, we isolated microglia from the cortical tissue of WT mice and incubated them with these pHrodo-conjugated synaptosomes. After a 2 h incubation, we observed that WT microglia engulfed a substantial quantity of synaptosomes from *dE9* mice without pioglitazone treatment (Fig. 4B). When synaptosomes from pioglitazone-treated *dE9* mice were applied to WT microglia, the engulfment was significantly suppressed, approaching levels close to those of the negative control, which consisted of microglia treated with cytochalasin D, an actin polymerization inhibitor that blocks phagocytosis (Fig. 4B).

Interestingly, within microglia, the level of C1q is tightly correlated with pHrodo-conjugated synaptosomes (Fig. 4B–D), which corroborates the findings on how C1q-tagging triggers synaptic loss.[7,8] On top of this, following pioglitazone treatment, we observed a significant reduction in C1q volumes in microglia (Fig. 4C). Combined with the reduced C1q in *dE9* synaptosomes (Fig. 3E and F), this suggests the suppressive effect of pioglitazone on the C1q-tagging at synapses.

Taken together, these findings indicate that pioglitazone mitigates the AD-induced synaptic loss by suppressing the C1q-tagging at synapses, thereby reducing microglial engulfment of synaptic materials.

Discussion

In this study, we demonstrated that pioglitazone, a PPAR-γ agonist, can alleviate synaptic loss at the early stage of AD pathology in *dE9* mice, a well-established amyloid-β AD mouse model. In particular, we found that after 4 weeks of pioglitazone treatment, dendritic spines close to amyloid-β plaques in the *dE9* cortex maintained a relatively higher density compared with those from untreated *dE9* mice. This is attributed mainly to enhanced resistance of dendritic spines to amyloid-β plaques and their relatively higher growth rate. In line with this, we observed that following pioglitazone treatment, plaque-surrounding microglia in the *dE9* cortex exhibited a reduced volume of lysosomes containing fewer postsynaptic compartments, indicating a dampened engulfment process. Upon further investigation, we found that, based on pioglitazone treatment, less C1q was detected in isolated *dE9* synaptosomes, suggesting reduced C1q deposition. As validated in subsequent experiments, synaptosomes with lower C1q levels were engulfed less when incubated with microglia from WT mice. Taken together, these findings provide both observational evidence and mechanistic proof supporting that pioglitazone treatment ameliorates amyloid-associated synaptic loss by reducing C1q deposition at synapses (Supplementary Fig. 2).

Given that the majority of pioglitazone-related studies have focused on its anti-inflammatory properties,[22-24] this is the first study to focus on how pioglitazone directly modulates the central piece of the immune system (the complement cascade) within the CNS. Our study provides evidence supporting pioglitazone and the related PPAR-γ pathway as potential therapeutic targets for preserving synapses in AD and other neurodegenerative diseases.

It is not new to investigate the therapeutic potential of pioglitazone in treatment of AD. As mentioned above, preclinical and clinical trials examining pioglitazone (or rosiglitazone) have produced variable results. Specifically, most of the preclinical studies using animal models demonstrated favourable effects of pioglitazone in halting AD progression,[12,25-32] whereas clinical studies with the same drugs have yielded inconclusive or contentious results.[33-38] There are many possible explanations for this disparity, including patient stratification, subpopulation heterogeneity and co-pathologies. One likely reason is the stage of the disease at which pioglitazone or other PPAR-γ agonists are administered. In both animal and human studies, most positive therapeutic effects are observed from animals with less advanced pathology[25-32] or human participants with mild to moderate levels of dementia (e.g. Mini-Mental State Examination > 20).[33,35,37,38] This is consistent with our findings that the beneficial effects of pioglitazone or similar PPAR-γ agonists are maximized when administered at the early stage of amyloid pathology, before widespread synaptic and neuronal loss occurs. In addition, our observation also aligns with a recent case report that emphasizes the importance of early therapeutic intervention in AD,[39] ideally before cognitive impairment manifests.

Given that early intervention with pioglitazone or other PPAR-γ agonists has demonstrated benefits for AD patients, it is essential to identify disease progression at the earliest possible stage. The current widely accepted ATN framework (A = amyloid pathology, T = tau pathology, N = neurodegeneration)[40] for AD diagnosis becomes most prominent in the relatively advanced stages of the disease. Therefore, there is a need for more time-sensitive measures, particularly those reflecting early AD pathology, such as synaptic damage and aberrant microglial activity. For synapse detection, recent studies show that several PET ligands targeting synaptic markers, such as synaptic vesicle glycoprotein 2A (SV2A),[41] can be used in humans. Additionally, C1q in CSF could also serve as a biomarker for synaptic damage, because both our findings and previous studies[7,42-44] report excessive C1q accumulation along with synaptic loss in early AD. For microglial measurements, earlier research also indicates that PET ligands targeting the 18 kDa translocator protein (TSPO),[45,46] or triggering receptor expressed on myeloid cells 2 (TREM2),[47] can be used to determine disease-associated microglial states. Collectively, these novel biomarkers will help to facilitate timely interventions, such as pioglitazone administration, to minimize synaptic loss at the earliest possible AD stage.

Despite the above-described findings, we acknowledge several limitations in this study. For instance, the precise mechanism underlying PPAR-γ-mediated modulation of C1q remains unclear. Early studies on diabetes have demonstrated that PPAR-γ agonists, such as pioglitazone or rosiglitazone, can reduce the binding ability of C1q to adiponectin, a protein that is widely recognized for its anti-diabetic and anti-inflammatory properties.[48,49] Although these results pertain to peripheral systems, when considered alongside our findings, they suggest that pioglitazone or the PPAR-γ pathway might also play a role in modulating the upstream phase of the C1q-binding and C1q-tagging process in the CNS. However, it remains to be elucidated whether this modulation involves direct protein–protein interactions or stems from certain common structural properties of PPAR-γ agonists.

Furthermore, as we strived to minimize variables and focus solely on pioglitazone-induced alterations at synapses, we isolated synaptosomes from the mouse brains. Earlier research has already indicated multiple potential sources of synaptic C1q deposition, such as microglia and astrocytes.[50,51] As a result, we cannot entirely rule out the involvement of other key elements in the CNS, e.g. glial cells and their interactions, in the pioglitazone-induced alterations of synaptic C1q. Further studies are required to explore whether and how these glial cells participate in the regulation of synaptic C1q following pioglitazone treatment.

Downloaded from https://academic.oup.com/brain/article/149/2/668/8380271 by Deutsches Zentrum fur Neurodegenerative Erkrankungen DZNE user on 26 February 2026

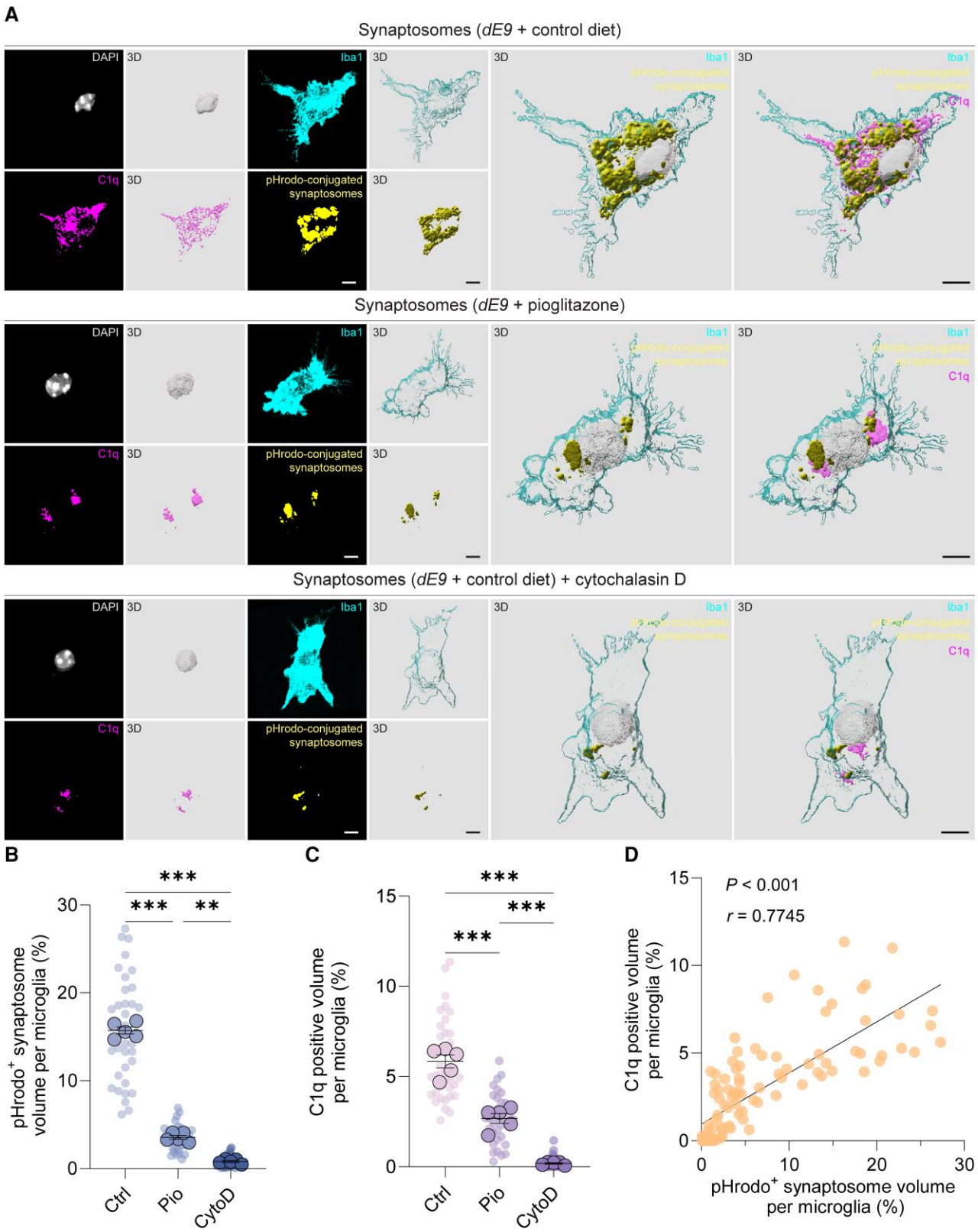

Figure 4 Pioglitazone reduces microglial engulfment of synapses by suppressing synaptic C1q-tagging. (**A**) Representative images and quantification of pHrodo-labelled synaptosome uptake by primary microglia isolated from wild-type (WT) mice. Microglia readily engulf synaptosomes derived from untreated *dE9* mice, whereas synaptosomes from pioglitazone-treated *dE9* mice show significantly reduced uptake. Cytochalasin D-treated microglia serve as a negative control for phagocytosis. (**B**) Quantification of synaptosome engulfment by microglia. Synaptosomes were isolated from control diet-treated and pioglitazone-treated *dE9* mice. Cytochalasin D treatment served as a negative control. (**C**) Quantification of C1q volume within microglia. (**D**) Correlation analysis showing a positive relationship between microglial C1q$^+$ volume and the amount of engulfed synaptosomes (Pearson's r = 0.7745, $P < 0.001$). $n = 5$ mice per group. Data are presented as the mean ± standard error of the mean. One-way ANOVA followed by Bonferroni's multiple comparisons test [**B**: $F(2,12) = 833.5$, $P < 0.001$; **C**: $F(2,12) = 116.1$, $P < 0.001$]. $^{**}P < 0.01$, $^{***}P < 0.001$. Scale bars: 5 μm in **A**.

Downloaded from https://academic.oup.com/brain/article/149/2/668/8380271 by Deutsches Zentrum fur Neurodegenerative Erkrankungen DZNE user on 26 February 2026

In addition, this study primarily examined molecular and structural alterations of synapses close to amyloid-β plaques in early AD. Although it is widely accepted that synapses serve as the underpinning of cognitive processes,[52-54] it remains questionable whether the pioglitazone-induced synaptic changes around amyloid-β plaques eventually translate into visible behavioural outcomes. One crucial factor to consider here is the stage of AD. Given that we used *dE9* mice at their earliest AD stage, the structural pathology is less likely to be reflected in the functional aspects, i.e. behaviours. Therefore, future investigations should extend the duration of pioglitazone treatment to encompass the onset of behavioural pathology in the animal model and observe outcomes over a longer treatment period. Moreover, the *dE9* model lacks tauopathy, a crucial component of AD-associated cognitive decline.[55,56] Although previous studies have shown that pioglitazone intervention is not effective on neuronal tau in singular tauopathy,[57] it remains to be explored how pioglitazone might preserve synapses in a similar pathology or, ideally, in a combined pathology of both amyloid-β and tau. Collectively, these approaches would allow for a more comprehensive study of the functional consequences of pioglitazone administration in AD.

Another limitation of this study is of a more practical nature. Here, we administered pioglitazone using an *ad libitum* approach. Although this method is widely used and we closely monitored the food consumption of the mice, it remains a concern that unwanted variations could arise owing to the unquantifiable nature of this approach. Therefore, in future studies, for bringing pioglitazone use closer to clinical practice, more accurate yet gentle drug administration methods suitable for long-term use, such as infusion pump implantation,[58,59] should be used.

Conclusion

In conclusion, our study highlights the protective effects of pioglitazone on AD-associated synaptic pathology at amyloid-β plaques. We unveiled a previously underexplored mechanism by which pioglitazone reduces synaptic C1q deposition, thereby preventing its removal by microglia. Given that synaptic function is fundamental to cognitive performance, our findings suggest that pioglitazone treatment might offer clinical benefits by slowing cognitive decline in AD. This is particularly significant given the current bottleneck of AD drugs in improving cognitive functions.[60,61] Moreover, considering that pioglitazone is widely used in clinical practice and has a well-established safety profile, our findings are highly translational, because the application of pioglitazone can be extended smoothly from its conventional indications to AD. Collectively, our study calls for a re-evaluation of pioglitazone and other PPAR-γ agonists as potential clinical interventions for early-stage treatment of cognitive decline in AD and other neurodegenerative diseases characterized by synaptic loss.

Data availability

The raw data supporting the findings of this study are available from the corresponding author upon reasonable request.

Acknowledgements

We thank Eric Griessinger and Katharina Bayer for their technical support and assistance with animal care.

Funding

This work was funded by the Deutsche Forschungsgemeinschaft (DFG, German Research Foundation) (DFG/ID 511905387 to Y.S.; FOR 2858/ID 422181340 to J.H.; EXC 2145/ID 390857198 to J.H.; ID 497637663 to J.H.) and Verein zur Förderung von Wissenschaft und Forschung an der Medizinischen Fakultät der LMU München (WiFoMed) (ID 8200676 to Y.S.).

Competing interests

The authors report no competing interests.

Supplementary material

Supplementary material is available at *Brain* online.

References

1. Aisen PS, Davis KL. Inflammatory mechanisms in Alzheimer's disease: Implications for therapy. *Am J Psychiatry*. 1994;151:1105-1113.
2. Akiyama H, Barger S, Barnum S, et al. Inflammation and Alzheimer's disease. *Neurobiol Aging*. 2000;21:383-421.
3. Hansen DV, Hanson JE, Sheng M. Microglia in Alzheimer's disease. *J Cell Biol*. 2018;217:459-472.
4. Rajendran L, Paolicelli RC. Microglia-mediated synapse loss in Alzheimer's disease. *J Neurosci*. 2018;38:2911-2919.
5. Sze CI, Troncoso JC, Kawas C, Mouton P, Price DL, Martin LJ. Loss of the presynaptic vesicle protein synaptophysin in hippocampus correlates with cognitive decline in Alzheimer disease. *J Neuropathol Exp Neurol*. 1997;56:933-944.
6. Terry RD, Masliah E, Salmon DP, et al. Physical basis of cognitive alterations in Alzheimer's disease: Synapse loss is the major correlate of cognitive impairment. *Ann Neurol*. 1991;30:572-580.
7. Hong S, Beja-Glasser VF, Nfonoyim BM, et al. Complement and microglia mediate early synapse loss in Alzheimer mouse models. *Science*. 2016;352:712-716.
8. Stevens B, Allen NJ, Vazquez LE, et al. The classical complement cascade mediates CNS synapse elimination. *Cell*. 2007;131:1164-1178.
9. Kishore U, Reid KB. C1q: Structure, function, and receptors. *Immunopharmacology*. 2000;49:159-170.
10. Woodburn SC, Bollinger JL, Wohleb ES. The semantics of microglia activation: Neuroinflammation, homeostasis, and stress. *J Neuroinflammation*. 2021;18:258.
11. Aisen PS. The potential of anti-inflammatory drugs for the treatment of Alzheimer's disease. *Lancet Neurol*. 2002;1:279-284.
12. Heneka MT, Sastre M, Dumitrescu-Ozimek L, et al. Acute treatment with the PPAR-γ agonist pioglitazone and ibuprofen reduces glial inflammation and Aβ1–42 levels in APPV717I transgenic mice. *Brain*. 2005;128(Pt 6):1442-1453.
13. Zhao Q, Wu X, Yan S, et al. The antidepressant-like effects of pioglitazone in a chronic mild stress mouse model are associated with PPAR-γ-mediated alteration of microglial activation phenotypes. *J Neuroinflammation*. 2016;13:259.
14. Searcy JL, Phelps JT, Pancani T, et al. Long-term pioglitazone treatment improves learning and attenuates pathological markers in a mouse model of Alzheimer's disease. *J Alzheimers Dis*. 2012;30:943-961.
15. Seok H, Lee M, Shin E, et al. Low-dose pioglitazone can ameliorate learning and memory impairment in a mouse model of

Downloaded from https://academic.oup.com/brain/article/149/2/668/8380271 by Deutsches Zentrum fur Neurodegenerative Erkrankungen DZNE user on 26 February 2026

dementia by increasing LRP1 expression in the hippocampus. *Sci Rep*. 2019;9:4414.
16. Jankowsky JL, Fadale DJ, Anderson J, et al. Mutant presenilins specifically elevate the levels of the 42 residue β-amyloid peptide *in vivo*: Evidence for augmentation of a 42-specific γ secretase. *Hum Mol Genet*. 2004;13:159-170.
17. Shi Y, Cui M, Blume T, Herms J. Intravital imaging and analysis of the structural plasticity of dendritic spines in multiple brain regions. In: Lübke JHR, Rollenhagen A, eds. *New aspects in analyzing the synaptic organization of the brain*. Springer US; 2024:395-430.
18. Jackson RJ, Rudinskiy N, Herrmann AG, et al. Human tau increases amyloid β plaque size but not amyloid β-mediated synapse loss in a novel mouse model of Alzheimer's disease. *Eur J Neurosci*. 2016;44:3056-3066.
19. Zou C, Shi Y, Ohli J, Schüller U, Dorostkar MM, Herms J. Neuroinflammation impairs adaptive structural plasticity of dendritic spines in a preclinical model of Alzheimer's disease. *Acta Neuropathol*. 2016;131:235-246.
20. Feng G, Mellor RH, Bernstein M, et al. Imaging neuronal subsets in transgenic mice expressing multiple spectral variants of GFP. *Neuron*. 2000;28:41-51.
21. Dejanovic B, Wu T, Tsai MC, et al. Complement C1q-dependent excitatory and inhibitory synapse elimination by astrocytes and microglia in Alzheimer's disease mouse models. *Nat Aging*. 2022;2:837-850.
22. Baagar K, Alessa T, Abu-Farha M, et al. Effect of pioglitazone on inflammatory response and clinical outcome in T2DM patients with COVID-19: A randomized multicenter double-blind clinical trial. *Front Immunol*. 2024;15:1369918.
23. Nasrabadi ME, Al-Harrasi A, Mohammadi S, Zarif Azam Kardani F, Rahmati M, Memarian A. Pioglitazone as a potential modulator in autoimmune diseases: A review on its effects in systemic lupus erythematosus, psoriasis, inflammatory bowel disease, and multiple sclerosis. *Expert Rev Clin Immunol*. 2025;21:5-15.
24. Zhang WY, Schwartz EA, Permana PA, Reaven PD. Pioglitazone inhibits the expression of inflammatory cytokines from both monocytes and lymphocytes in patients with impaired glucose tolerance. *Arterioscler Thromb Vasc Biol*. 2008;28:2312-2318.
25. Badhwar A, Lerch JP, Hamel E, Sled JG. Impaired structural correlates of memory in Alzheimer's disease mice. *Neuroimage Clin*. 2013;3:290-300.
26. Escribano L, Simón AM, Pérez-Mediavilla A, Salazar-Colocho P, Río JD, Frechilla D. Rosiglitazone reverses memory decline and hippocampal glucocorticoid receptor down-regulation in an Alzheimer's disease mouse model. *Biochem Biophys Res Commun*. 2009;379:406-410.
27. Mandrekar-Colucci S, Karlo JC, Landreth GE. Mechanisms underlying the rapid peroxisome proliferator-activated receptor-γ-mediated amyloid clearance and reversal of cognitive deficits in a murine model of Alzheimer's disease. *J Neurosci*. 2012;32:10117-10128.
28. Nenov MN, Laezza F, Haidacher SJ, et al. Cognitive enhancing treatment with a PPAR-γ agonist normalizes dentate granule cell presynaptic function in Tg2576 APP mice. *J Neurosci*. 2014;34:1028-1036.
29. Pedersen WA, McMillan PJ, Kulstad JJ, Leverenz JB, Craft S, Haynatzki GR. Rosiglitazone attenuates learning and memory deficits in Tg2576 Alzheimer mice. *Exp Neurol*. 2006;199:265-273.
30. Rodriguez-Rivera J, Denner L, Dineley KT. Rosiglitazone reversal of Tg2576 cognitive deficits is independent of peripheral gluco-regulatory status. *Behav Brain Res*. 2011;216:255-261.
31. Skerrett R, Pellegrino MP, Casali BT, Taraboanta L, Landreth GE. Combined liver X receptor/peroxisome proliferator-activated receptor γ agonist treatment reduces amyloid beta levels and improves behavior in amyloid precursor protein/presenilin 1 mice. *J Biol Chem*. 2015;290:21591-21602.
32. Toba J, Nikkuni M, Ishizeki M, et al. PPAR-γ agonist pioglitazone improves cerebellar dysfunction at pre-Aβ deposition stage in APPswe/PS1dE9 Alzheimer's disease model mice. *Biochem Biophys Res Commun*. 2016;473:1039-1044.
33. Abbatecola AM, Lattanzio F, Molinari AM, et al. Rosiglitazone and cognitive stability in older individuals with type 2 diabetes and mild cognitive impairment. *Diabetes Care*. 2010;33:1706-1711.
34. Gold M, Alderton C, Zvartau-Hind M, et al. Rosiglitazone monotherapy in mild-to-moderate Alzheimer's disease: Results from a randomized, double-blind, placebo-controlled phase III study. *Dement Geriatr Cogn Disord*. 2010;30:131-146.
35. Hanyu H, Sato T, Sakurai H, Iwamoto T. The role of tumor necrosis factor-alpha in cognitive improvement after peroxisome proliferator-activator receptor γ agonist pioglitazone treatment in Alzheimer's disease. *J Am Geriatr Soc*. 2010;58:1000-1001.
36. Harrington C, Sawchak S, Chiang C, et al. Rosiglitazone does not improve cognition or global function when used as adjunctive therapy to AChE inhibitors in mild-to-moderate Alzheimer's disease: Two phase 3 studies. *Curr Alzheimer Res*. 2011;8:592-606.
37. Sato T, Hanyu H, Hirao K, Kanetaka H, Sakurai H, Iwamoto T. Efficacy of PPAR-γ agonist pioglitazone in mild Alzheimer disease. *Neurobiol Aging*. 2011;32:1626-1633.
38. Watson GS, Cholerton BA, Reger MA, et al. Preserved cognition in patients with early Alzheimer disease and amnestic mild cognitive impairment during treatment with rosiglitazone: A preliminary study. *Am J Geriatr Psychiatry*. 2005;13:950-958.
39. Read S, Wu P, Biscow M. Sustained 4-year cognitive and functional response in early Alzheimer's disease with pioglitazone. *J Am Geriatr Soc*. 2014;62:584-586.
40. Knopman DS, Haeberlein SB, Carrillo MC, et al. The National Institute on Aging and the Alzheimer's Association research framework for Alzheimer's disease: Perspectives from the research roundtable. *Alzheimers Dement*. 2018;14:563-575.
41. Visser M, O'Brien JT, Mak E. In vivo imaging of synaptic density in neurodegenerative disorders with positron emission tomography: A systematic review. *Ageing Res Rev*. 2024;94:102197.
42. Fonseca MI, Kawas CH, Troncoso JC, Tenner AJ. Neuronal localization of C1q in preclinical Alzheimer's disease. *Neurobiol Dis*. 2004;15:40-46.
43. van de Bovenkamp FS, Dijkstra DJ, van Kooten C, Gelderman KA, Trouw LA. Circulating C1q levels in health and disease, more than just a biomarker. *Mol Immunol*. 2021;140:206-216.
44. Wen L, Bi D, Shen Y. Complement-mediated synapse loss in Alzheimer's disease: Mechanisms and involvement of risk factors. *Trends Neurosci*. 2024;47:135-149.
45. Rossano SM, Johnson AS, Smith A, et al. Microglia measured by TSPO PET are associated with Alzheimer's disease pathology and mediate key steps in a disease progression model. *Alzheimers Dement*. 2024;20:2397-2407.
46. Wijesinghe SS, Rowe JB, Mason HD, et al. Post-mortem validation of *in vivo* TSPO PET as a microglial biomarker. *Brain*. 2025;148:1904-1910.
47. Shojaei M, Schaefer R, Schlepckow K, et al. PET imaging of microglia in Alzheimer's disease using copper-64 labeled TREM2 antibodies. *Theranostics*. 2024;14:6319-6336.
48. Nakatsuji H, Kishida K, Kobayashi H, Funahashi T, Shimomura I, The Senri Study II Group. Three-month treatment with pioglitazone reduces circulating C1q-binding adiponectin complex to total-adiponectin ratio, without changes in body mass index, in people with type 2 diabetes. *Diabetes Res Clin Pract*. 2013;99:e14-e17.

Downloaded from https://academic.oup.com/brain/article/149/2/668/8380271 by Deutsches Zentrum fur Neurodegenerative Erkrankungen DZNE user on 26 February 2026

49. Wong GW, Krawczyk SA, Kitidis-Mitrokostas C, Revett T, Gimeno R, Lodish HF. Molecular, biochemical and functional characterizations of C1q/TNF family members: Adipose-tissue-selective expression patterns, regulation by PPAR-γ agonist, cysteine-mediated oligomerizations, combinatorial associations and metabolic functions. *Biochem J*. 2008; 416:161-177.
50. Rambach G, Maier H, Vago G, et al. Complement induction and complement evasion in patients with cerebral aspergillosis. *Microbes Infect*. 2008;10:1567–1576.
51. Scott-Hewitt N, Mahoney M, Huang Y, et al. Microglial-derived C1q integrates into neuronal ribonucleoprotein complexes and impacts protein homeostasis in the aging brain. *Cell*. 2024; 187:4193-4212.e24.
52. Citri A, Malenka RC. Synaptic plasticity: Multiple forms, functions, and mechanisms. *Neuropsychopharmacology*. 2008;33: 18-41.
53. Hering H, Sheng M. Dendritic spines: Structure, dynamics and regulation. *Nat Rev Neurosci*. 2001;2:880-888.
54. Magee JC, Grienberger C. Synaptic plasticity forms and functions. *Annu Rev Neurosci*. 2020;43:95-117.
55. Ossenkoppele R, Salvadó G, Janelidze S, et al. Plasma p-tau217 and tau-PET predict future cognitive decline among cognitively unimpaired individuals: Implications for clinical trials. *Nat Aging*. 2025;5:883–896.
56. Cano A, Capdevila M, Puerta R, et al. Clinical value of plasma pTau181 to predict Alzheimer's disease pathology in a large real-world cohort of a memory clinic. *EBioMedicine*. 2024;108: 105345.
57. Kunze LH, Ruch F, Biechele G, et al. Long-term pioglitazone treatment has no significant impact on microglial activation and tau pathology in P301S mice. *Int J Mol Sci*. 2023;24:10106.
58. Abe C, Tashiro T, Tanaka K, Ogihara R, Morita H. A novel type of implantable and programmable infusion pump for small laboratory animals. *J Pharmacol Toxicol Methods*. 2009;59:7-12.
59. Liu S, Miyoshi M. Long-term constant subcutaneous drug administration. *Methods Mol Biol*. 2024;2766:31-36.
60. Cummings J, Cohen S, Murphy J, et al. Evaluation of cognitive, functional, and behavioral effects observed in EMERGE, a phase 3 trial of aducanumab in people with early Alzheimer's disease. *Alzheimers Dement*. 2025;21:e70224.
61. McDade E, Cummings JL, Dhadda S, et al. Lecanemab in patients with early Alzheimer's disease: Detailed results on biomarker, cognitive, and clinical effects from the randomized and open-label extension of the phase 2 proof-of-concept study. *Alzheimers Res Ther*. 2022;14:191.

Downloaded from https://academic.oup.com/brain/article/149/2/668/8380271 by Deutsches Zentrum fur Neurodegenerative Erkrankungen DZNE user on 26 February 2026